Open-Ended Dielectric–Filled Waveguide Antenna for Underwater Usage

Michael Sporer, Robert Weigel and Alexander Koelpin
Institute for Electronics Engineering, Friedrich-Alexander University of Erlangen-Nuremberg,
Cauerstr. 9, D-91058 Erlangen, Germany
Email: {michael.sporer, robert.weigel, alexander.koelpin}@fau.de

***Abstract*—In wireless short–range underwater communication a trend towards higher operating frequencies and bandwidth can be noticed in order to increase channel capacity and throughput. For launching electromagnetic waves typically low–directive wire antennas are employed. In this work a new kind of underwater antenna is presented for the 2.4 GHz industrial, scientific and medical (ISM) band, based on a dielectric filled open–ended waveguide. The antenna is designed as impedance matching transformer allowing a connection of conventional 50 Ω coaxial cables. The measured 10 dB bandwidth in fresh water is approx. 550 MHz (22 %). Compared to a conventional monopole antenna an increase in receive power of approx. 14 dB can be achieved.**

I. Introduction

Because of the high attenuation of electromagnetic (EM) waves with increasing frequency in water long–range underwater communication is limited to very low frequency (VLF) and extremely low frequency (ELF) bands. The main drawbacks, i.e. huge antenna size, low bandwidth, low data rates, must be accepted.

Recently, emerging fields of application can be noticed with focus on data rate rather than on range. An example is communication between autonomous underwater vehicles (AUV) and unmanned underwater platforms (UUP) for monitoring, controlling and retrieving sensor data [1]. It is likely for the data rate to increase with rising complexity and performance of vehicles and sensors, e.g. high–resolution video sensors. Communication has to be wireless in order to achieve efficiency, reliability, and robustness.

Therefore, there are growing efforts to increase the frequency to the MHz and even GHz range in order to rise bandwidth and channel capacity. Additionally, modern modulation schemes (e.g. orthogonal frequency division multiplex (OFDM)) in combination with multiple input multiple output (MIMO) techniques are analyzed for underwater utilization in order to enhance throughput [2], [3].

Since providing the interface between wired and wireless wave propagation antennas are a core component in an underwater communication system. However, antennas intended of air usage can generally not be applied in underwater environments without changing antenna attributes (e.g. input impedance or resonance frequency) because of the significant different electromagnetic properties of the two propagation media. Typically, isolated wire antennas are shown to be efficient underwater radiators and are used in the majority of systems.

E.g. Lucas et al propose in [4] an open-ended parallel wire transmission line immersed in a PVC barrel filled with destilled water for investigating propagation of EM waves in seawater in the $1 - 100\,\mathrm{MHz}$ frequency range. Additionally, the authors studied dipole antennas encased in PVC filled with pure water and isolated wire loop antennas [5]. Wire antennas are also employed by other researchers, e.g. Al-Shamma'a et al (dipole, monopole, loop antennas) for 0.1-60 MHz, 433 MHz and 2.4 GHz [6]–[8]. Zhang et al propose loop and j–type vibrator antennas (7 MHz and 30 MHz) [9], [10]. Recently in [11] a dual–band double–spiral coil antenna is presented allowing both power transfer at 1 MHz and signal communication at 90 MHz. In [12] a microstrip bow–tie antenna is shown (433 MHz) and in [13] a Wi–Fi antenna (2.4 GHz) based on a tin–can as buffer cavity.

In the following we first give a review of electromagnetic properties of water (i.e. complex permittivity, wave attenuation, free space impedance). Next, we present a new kind of underwater antenna based on a dielectric filled open–ended waveguide intended for the 2.4 GHz industrial, scientific, medical (ISM) frequency band.

A. Electromagnetic properties of water

Water molecules have a distinct dipole character and therefore show strong polarizability. This results in relatively high dielectric permittivity of fluid water generally depending on frequency f, temperature T (in °C) and conductivity σ, caused by a concentration S (in ppt) of additives (e.g. salt), if any. The complex relative permittivity ε_r can be described by the second–order Debye model

$$\varepsilon_r(T,S,f) = \frac{\varepsilon_s(T,S) - \varepsilon_1(T,S)}{1 + jf/f_1(T,S)} + \frac{\varepsilon_1(T,S) - \varepsilon_\infty(T,S)}{1 + jf/f_2(T,S)} + \varepsilon_\infty(T,S) + j \cdot \frac{\sigma(T,S)}{2\pi\varepsilon_0 f} = \varepsilon' - j\varepsilon'' \qquad (1)$$

with ε_0, ε_s, ε_1, ε_∞ being the vacuum, static, immediate and asymptotic dielectric permittivities. The frequencies f_1 and f_2 denote the first and second Debye relaxation frequencies in GHz. In [14] empirical formulas are given for the parameters in case of salt as additive.

Fig. 1 and 2 show the real (ε') and imaginary (ε'') part of the relative permittivity of water between 0.01–100 GHz and for different temperatures and salinities, respectively. Both, real and imaginary parts show a strong variation especially

around the relaxation frequency of water ($\approx$ 20 GHz). For lower frequencies ε_r' decreases with increasing temperature and salinity. Note the strong dependency of ε_r'' on salinity for low frequencies.

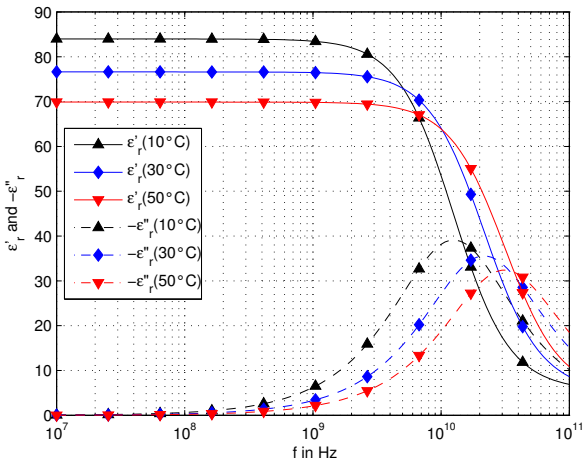

Fig. 1. Real (solid line) and imaginary (dashed line) part of the relative permittivity of destilled water ($S = 0$) between 0.01–100 GHz for different temperatures

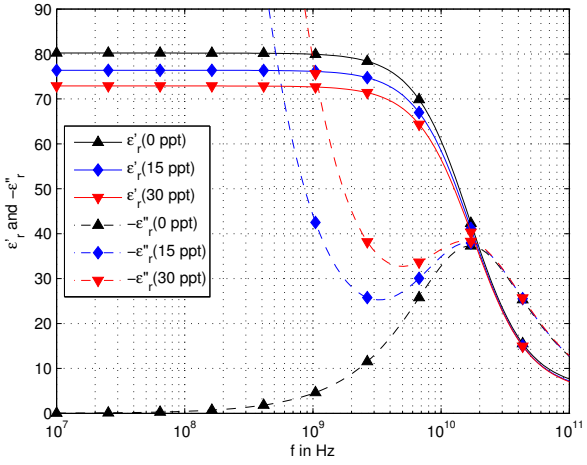

Fig. 2. Real (solid line) and imaginary (dashed line) part of the relative permittivity of water between 0.01–100 GHz for different salinities at 20°C

Assuming a negligible magnetic polarizability ($\mu = \mu_0$) of water with μ_0 being the vacuum permeability the wavenumber k and the complex intrinsic impedance η become

$$k = \beta - j\alpha = 2\pi f\sqrt{\mu_0\varepsilon_0(\varepsilon_r' - j\varepsilon_r'')} \tag{2}$$

$$\eta = \sqrt{\frac{\mu_0}{\varepsilon_0(\varepsilon_r' - j\varepsilon_r'')}} \tag{3}$$

with β and α being the phase and the attenuation constant [15]. Fig. 3 shows real (Re{}) and imaginary (Im{}) part of η between 0.1–10 GHz for different temperatures and salinities. In case of distilled water $Re\{\eta\}$ remains nearly constant (40–45 Ω) whereas $Im\{\eta\}$ varies between 0–14 Ω with frequency and temperature. The influence of temperature increases with rising frequency. Salinity shows strong impact on both real and imaginary part particularly for low frequencies.

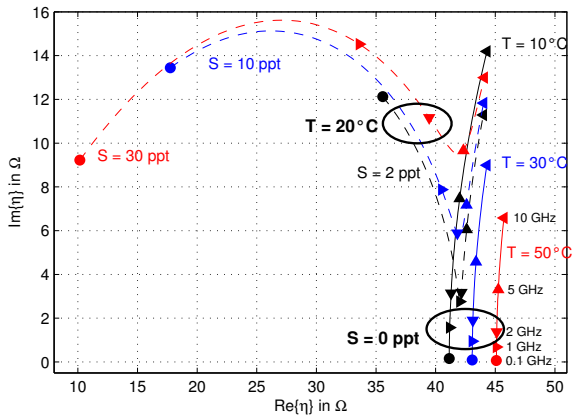

Fig. 3. Real and imaginary part of the intrinsic impedance of water between 0.1–10 GHz for different temperatures (solid lines) and salinities (dashed lines). Markers indicate the frequency (see labels in the bottom right–hand corner).

The power per unit area of a plane wave propagating a distance z and thus the power attenuation in dB per meter become

$$P(z) = P(0) \cdot e^{-2\alpha z} \tag{4}$$

$$A_{dB} = -10\log_{10}\left(\frac{P(z)}{P(0)}\right) = 20\log_{10}(e)\alpha z \tag{5}$$

shown in Fig. 4 between 0.01–10 GHz for different salinitites and temperatures.

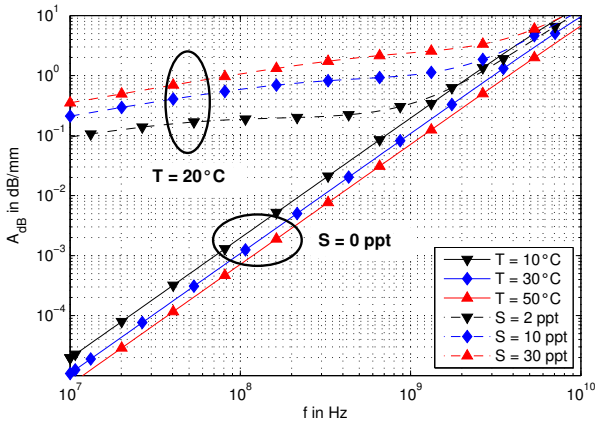

Fig. 4. Attenuation of a plane wave propagating through water of different salinities (dashed lines) and temperatures (solid lines) between 0.01–10 GHz.

The negative impact of salinity on attenuation for frequencies less than approx. 3 GHz even for small concentrations is clearly visible. Regarding higher frequencies the curves of varying salinity asymptotically approach those of distilled water.

Since an antenna can be considered as impedance matching transformer transforming the impedance of a guided wave into

the intrinsic impedance of the medium irradiated, knowledge about the latter is essential for successful antenna development (Equ. 3 and Fig. 3). In the following section we present an open–ended dielectric filled waveguide antenna for underwater use designed as impedance matching transformer.

B. Underwater Open–Ended Waveguide Antenna

In air, waveguide antennas, especially horn antennas, show great popularity at microwave frequencies because of their low–cost mechanical design, high bandwidth, and gain. A horn antenna consists of a metal waveguide flared out at its end in order to increase the area of the radiating aperture and thus directivity. Further, the taper gradually decreases the wave impedance (see Equ. 6) within the waveguide and thus transforms the impedance to the impedance of free space ($\eta_0 \approx 377\,\Omega$ in case of vacuum). The wave impedance $\eta_{wg}^{\varepsilon_r}$ of the dominant mode (H_{10}) of a rectangular dielectric–filled waveguide, the guided wavelength $\lambda_{wg}^{\varepsilon_r}$ and the cut–off frequency $f_c^{\varepsilon_r}$ are

$$\eta_{wg}^{\varepsilon_r} = \frac{\eta_0}{\sqrt{\varepsilon_r}} \cdot \left(\sqrt{1 - \left(\frac{f_c}{f} \right)^2} \right)^{-1} \tag{6}$$

$$\lambda_{wg}^{\varepsilon_r} = \frac{c_0}{f\sqrt{\varepsilon_r}} \cdot \left(\sqrt{1 - \left(\frac{f_c}{f} \right)^2} \right)^{-1} \tag{7}$$

$$f_c^{\varepsilon_r} = \frac{c_0}{\sqrt{\varepsilon_r}} \cdot \frac{1}{2a} \tag{8}$$

where ε_r, c_0 and a denote the relative permittivity of the dielectric, the speed of light in vaccuum and the length of the longest side of the waveguide, respectively [15].

Applying this concept to underwater application by using a water–filled horn with appropriate dimensions is imaginable. However, this would yield a low efficiency because of the high attenuation of the wave while travelling along the horn (typically a few wavelengths) even for distilled water. Alternatively, a low–lossy dielectric with permittivity similar to water can be used, though appropriate materials with high permittivities (typically ceramics) are difficult to handle.

Our solution consists of an open–ended waveguide filled with two dielectrics of different permittivities and a capacitive iris inbetween, as shown in Fig. 5.

Waveguide and iris are made of copper sheets and copper foil with thickness of 0.7 mm and 0.03 mm. The dielectrics are conventional printed circuit board (PCB) laminates stacked and glued together with epoxy resin. Precisely, RO3010 from Rogers cooperation and FR4 with corresponding permittivities of $\varepsilon_r^{ro} = 10$ and $\varepsilon_r^{fr4} = 4.5$ are used. For connecting a $50\,\Omega$ coaxial cable a conventional E–plane coax–to–waveguide transition with probe length $l_p = 15\,\mathrm{mm}$ is inserted. The inner dimensions of the waveguide are $a = 40\,\mathrm{mm}$, $b = 20\,\mathrm{mm}$ and $L = 31.8\,\mathrm{mm}$, the iris opening is 7 mm.

Fig. 6 shows the corresponding equivalent circuit diagram. The design is based on two waveguide sections. The first section (RO3010 and capacitive iris) performs the impedance

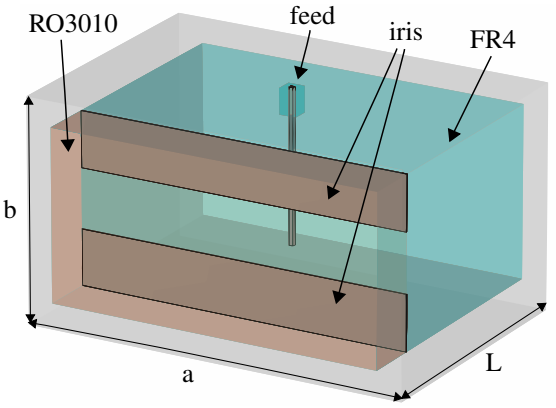

Fig. 5. Simulation model of the proposed antenna

transformation from water into the impedance of the second, FR4–filled section ($262\,\Omega$). The second section realizes the waveguide–to–coax transition. For simulations, the impedance of water is assumed as $\eta_w = 43\,\Omega$ corresponding to distilled water at the design frequency.

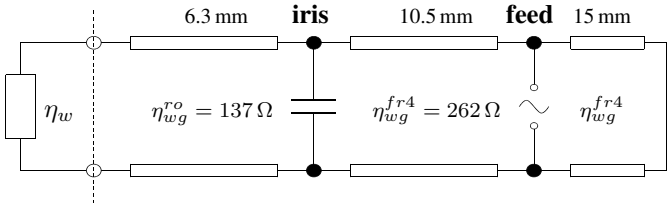

Fig. 6. Equivalent circuit diagram of the proposed antenna

The design was simulated using CST Microwave Studio and fabricated. Fig. 7 shows a photograph of the fabricated antenna with removed front for clarity.

Fig. 7. Photograph of the fabricated antenna. The front dielectic (RO3010) is removed for demonstration purposes.

The return loss was measured by holding the antenna into an aquarium (60x30x40 cm) filled with fresh water. Fig. 8 shows the simulated and the measured return loss. Despite a slight shift in resonant frequency, probably because of imprecise knowledge of ε_r^{fr4} there is a good agreement between simulation and measurement. The 10 dB bandwidth is approx. 550 MHz (22 %).

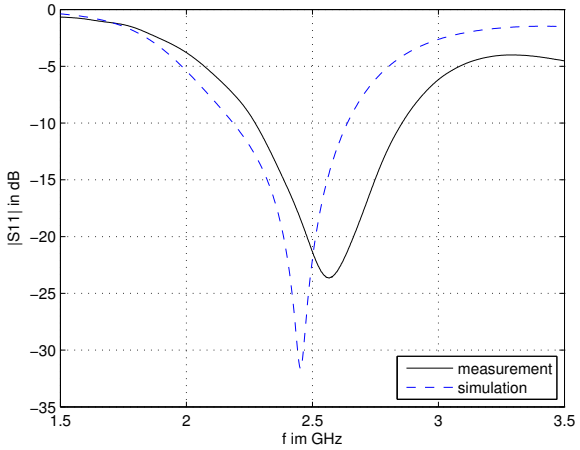

Fig. 8. Simulated (solid line) and measured (dashed line) return loss of the antenna in fresh water between 1.5–3.5 GHz

Additionally, for comparison and in order to evaluate antenna directivity distance measurements are performed. Firstly, the transmittance between two conventional monopole antennas with varying distance is studied by measurement of $|S_{21}|$ using a network analyzer. The monopole antennas are made of coax cables with 7 mm of the shielding stripped back from the end. The return loss is measured as 6.7 dB resulting in an additional loss of approx. 1.0 dB for each monopole antenna. Afterwards, the same measurements are carried out with one of the monopoles replaced by the proposed open–ended waveguide antenna. Results are shown in Fig. 9.

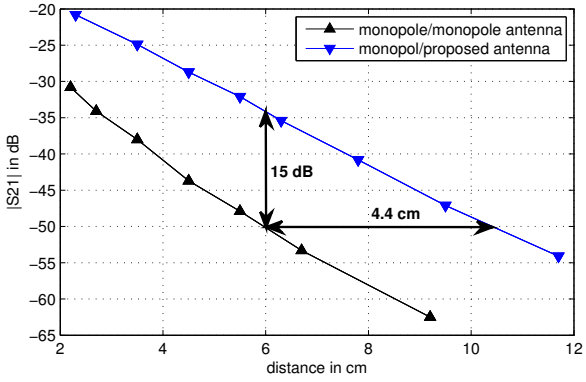

Fig. 9. Comparison of conventional monopole antenna and proposed antenna

Considering the additional return losses of the monopole antenna an increase of approx. $15\,\mathrm{dB} - 1\,\mathrm{dB} = 14\,\mathrm{dB}$ in receive power can be achieved using the proposed antenna which in turn extends the range for data transmission by approx. 4 cm.

II. Conclusion

In wireless underwater communication applications typically wire antennas are employed. This work presents a new kind of underwater antenna intended for short–range applications in the 2.4 GHz frequency band. The antenna is based on a open–ended waveguide filled with two dielectrics of different permittivities (FR4 and RO3010) and a capacitive iris inbetween. The design works as impedance matching transformer and provides a 50 Ω interface for connecting conventional coaxial cables. The antenna was developed using a commercial electromagnetic field simulation software applying the electromagnetic properties of water indicated in this work. For verification, experimental studies are carried out in fresh water showing a good agreement with the simulation. The antenna offers a 10 dB bandwidth of 550 MHz (22 %) and a high directivity. An increase in receive power of approx. 14 dB is achieved compared to a conventional monopole antenna.

Further investigations will be carried out in order to study the field distribution and the influence of salinity and temperature.

References

[1] T. Shaneyfelt, M. Joordens, K. Nagothu, and M. Jamshidi, "Rf communication between surface and underwater robotic swarms," in *Automation Congress, 2008. WAC 2008. World*, Sept 2008, pp. 1–6.

[2] B. Kelley, K. Manoj, and M. Jamshidi, "Broadband rf communications in underwater environments using multi-carrier modulation," in *Systems, Man and Cybernetics, 2009. SMC 2009. IEEE International Conference on*, Oct 2009, pp. 2303–2308.

[3] H. D. Trung and V. D. Nguyen, "An analysis of mimo-ofdm for underwater communications," in *Ultra Modern Telecommunications and Control Systems and Workshops (ICUMT), 2011 3rd International Congress on*, Oct 2011, pp. 1–5.

[4] C. Yip, A. Goudevenos, and J. Lucas, "Antenna design for the propagation of em waves in seawater," *Underwater Technology*, vol. 28, no. 1, pp. 11–20, 2008.

[5] J. Lucas and C. Yip, "A determination of the propagation of electromagnetic waves through seawater," *Underwater Technology*, vol. 27, no. 1, pp. 1–9, 2007.

[6] A. Shaw, A. Al-Shamma'a, S. Wylie, and D. Toal, "Experimental investigations of electromagnetic wave propagation in seawater," in *Microwave Conference, 2006. 36th European*, Sept 2006, pp. 572–575.

[7] A. Abdou, A. Shaw, A. Mason, A. Al-Shamma'a, S. Wylie, and J. Cullen, "Wireless sensor network for underwater communication," in *Wireless Sensor Systems (WSS 2012), IET Conference on*, June 2012, pp. 1–6.

[8] A. Al-Shamma'a, A. Shaw, and S. Saman, "Propagation of electromagnetic waves at mhz frequencies through seawater," *Antennas and Propagation, IEEE Transactions on*, vol. 52, no. 11, pp. 2843–2849, Nov 2004.

[9] Z. Hao, G. Dawei, Z. Guoping, and T. Gulliver, "The impact of antenna design and frequency on underwater wireless communications," in *Communications, Computers and Signal Processing (PacRim), 2011 IEEE Pacific Rim Conference on*, Aug 2011, pp. 868–872.

[10] H. Zhang and F. Meng, "Exploiting the skin effect using radio frequency communication in underwater communication," in *Industrial Control and Electronics Engineering (ICICEE), 2012 International Conference on*, Aug 2012, pp. 1150–1153.

[11] H. Fukuda, N. Kobayashi, K. Shizuno, S. Yoshida, M. Tanomura, and Y. Hama, "New concept of an electromagnetic usage for contactless communication and power transmission in the ocean," in *Underwater Technology Symposium (UT), 2013 IEEE International*, March 2013, pp. 1–4.

[12] A. A. Abdou, A. Mason, A. Al-Shamma'a, J. Cullen, S. Wylie, M. Diallo, and A. Shaw, "A matched bow-tie antenna at 433mhz for use in underwater wireless sensor networks," *Journal of Physics: Conference Series*, vol. 450, no. 1, pp. 12 048–12 054, 2013.

[13] H. Guarnizo Mendez, C. Gac, F. Le Pennec, and C. Person, "High performance underwater uhf radio antenna development," in *OCEANS, 2011 IEEE - Spain*, June 2011, pp. 1–5.

[14] T. Meissner and F. Wentz, "The complex dielectric constant of pure and sea water from microwave satellite observations," *Geoscience and Remote Sensing, IEEE Transactions on*, vol. 42, no. 9, pp. 1836–1849, Sept 2004.

[15] S. J. Orfanidis, *Electromagnetic waves and antennas*. ECE Department, Rutgers University, August 25, 2013.